The AAA+ protein Msp1 selects substrates by recognizing a hydrophobic mismatch between the substrate transmembrane domain and the lipid bilayer

Heidi L. Fresenius[1], Deepika Gaur[1], and Matthew L. Wohlever[1*]

Affiliations:
[1]Department of Chemistry & Biochemistry, University of Toledo, Toledo, OH, USA

*Correspondence should be addressed to MLW (matthew.wohlever@utoledo.edu)

Abstract:
An essential aspect of protein quality control is enzymatic removal of membrane proteins from the lipid bilayer. Failures in this essential cellular process are associated with neurodegenerative diseases and cancer. Msp1 is a AAA+ (ATPases Associated with diverse cellular Activities) protein that removes mistargeted proteins from the outer mitochondrial membrane (OMM). How Msp1 selectively recognizes and extracts substrates within the complex OMM ecosystem, and the role of the lipid bilayer on these processes is unknown. Here, we describe the development of fully defined, rapid, and quantitative extraction assay that retains physiological substrate selectivity. Using this new assay, we systematically modified both substrates and the lipid environment to demonstrate that Msp1 recognizes substrates by a hydrophobic mismatch between the substrate TMD and the lipid bilayer. We further demonstrate that the rate limiting step in Msp1 activity is extraction of the TMD from the lipid bilayer. Together, these results provide foundational insights into how the lipid bilayer influences AAA+ mediated membrane protein extraction.

Introduction:

A hallmark of eukaryotic cells is membrane bound organelles with each organelle characterized by unique protein and lipid compositions. As a foundational mechanism for organizing cellular reactions and signaling pathways, the cell devotes significant resources toward establishing and maintaining unique organelle proteomes and lipidomes. Despite the clear importance of targeting membrane proteins to the correct organelle, membrane protein trafficking and insertion pathways are surprisingly error prone and depend heavily on post-insertion quality control pathways to correct protein targeting errors.

One such pathway involves the AAA ATPase Msp1, which extracts proteins from the outer mitochondrial membrane (OMM) and peroxisome[1,2]. Msp1 substrates include endoplasmic reticulum (ER) tail anchored (TA) proteins that mislocalized to the OMM or peroxisomal TA proteins that are in stoichiometric excess of their binding partners[3]. Msp1 also helps relieve mitochondrial protein import stress by clearing stalled substrates from the TOM complex[4]. ATAD1, the human homolog of Msp1, serves an expanded role in membrane proteostasis by regulating AMPA receptor internalization and selectively removing the pro-apoptotic protein BIM from the OMM[5,6]. Loss of Msp1/ATAD1 lead to failures in oxidative phosphorylation, impaired fear conditioning, apoptotic priming, and enhanced susceptibility to proteotoxic stress. Loss of ATAD1 in mice or humans is lethal[7,8].

Given the clear health relevance, it is of paramount importance to understand how Msp1 recognizes substrates. In particular, it is unclear how Msp1 can selectively recognize mislocalized TA proteins from a large excess of properly localized mitochondrial proteins. There

are currently several competing models in the literature for how Msp1 recognizes substrates[9,10], however the role of the lipid bilayer in substrate recognition has been largely ignored. We previously used a reconstituted system to demonstrate that Msp1 is sufficient to recognize and extract a tail anchored protein from a fully defined lipid bilayer[11,12]. Furthermore, this reconstituted system showed physiological substrate selectivity as it specifically removed ER-TA proteins, but not the mitochondrial TA protein Fis1[6].

Here, we use a new and improved extraction assay to test the role of the substrate TMD and lipid bilayer in substrate extraction. We vary TMD length and bilayer thickness to demonstrate that Msp1 senses a hydrophobic mismatch between the substrate TMD and lipid bilayer to select substrates for extraction. We also demonstrate that a more fluid lipid bilayer allows for faster substrate extraction, suggesting that removal of a substrate from the lipid bilayer, rather than unfolding of cytosolic domains, is the rate limiting step in Msp1 activity. Together, these results demonstrate that the lipid bilayer plays a critical role in protein quality control and provide a detailed model for how Msp1 is able to selectively recognize and remove mislocalized membrane proteins from the far more abundant OMM resident proteins.

Results

Development of a more quantitative extraction assay

To observe potentially subtle differences in Msp1 activity, we completely redesigned the extraction assay. The new assay quantifies Msp1 extraction activity with the NanoLuc split luciferase system[13,14]. We cloned the 11-residue HiBiT sequence onto the C-terminus of our substrate, which is sequestered in the lumen of the liposome after reconstitution **(Figure 1A)**.

After reconstitution of substrate into pre-formed liposomes, the TA protein chaperones SGTA and calmodulin are added to remove any non-integrated substrate by immunoprecipitation **(Figure 1B)**. After this pre-clearing step, proper substrate orientation was validated by a protease protection assay that detects the HiBiT peptide **(Figure 1C)**. All of our substrates contain a thrombin protease site between the TMD and the HiBiT tag **(Figure 1A)**. Thrombin cleavage results in HiBiT peptide that is not resolvable by SDS PAGE/western blot. Addition of the thrombin protease led to a minimal loss of signal, whereas addition of both thrombin and the detergent Triton X-100 led to a complete loss of signal, demonstrating that the vast majority of substrate is properly oriented.

After reconstitution, the assay is initiated by adding ATP. Fresh SGTA and calmodulin are also added to capture extracted substrates. After a 30-minute incubation at 30° C, Msp1 activity is inhibited by chilling the reaction on ice[12] and then liposomes are pelleted by ultracentrifugation **(Figure 1B)**. We observed that the addition of an inert, His_6-tagged protein (His_6-MBP-ubiquitin) immediately prior to ultracentrifugation significantly reduces background activity, presumably by improving liposome pelleting **(Figure 1D)**. The supernatant is then mixed with LgBiT and the luciferase substrate furimazine and luminescence is measured on a plate reader. To quantify total extraction activity, we generated a standard curve by mixing liposomes with LgBiT, the luciferase reagent furimazine, and detergent, which leads to membrane permeabilization **(Figure 1E)**.

Another major change is that we used soluble Msp1 instead of full-length Msp1. We and others had previously demonstrated that the Msp1 TMD can be completely changed with no effect on Msp1 activity *in vivo*[3,12]. Similarly, we also demonstrated that soluble Msp1 retains robust and physiologically selective extraction activity *in vitro* if it is anchored to liposomes via a Ni-His interaction[6]. The use of soluble Msp1 dramatically simplifies the reconstitution process

as only the substrate protein needs to be reconstituted rather than co-reconstitution of substrate and six copies of Msp1. This allows us to directly compare extraction efficiency between different liposomes as we have eliminated any potential effects of liposomes on Msp1 reconstitution efficiency.

We tested substrate extraction with our standard model substrate, Sumo-Sec22, and standard liposome preparation, which mimics the outer mitochondrial membrane[15]. We observed robust, ATP dependent extraction **(Figure 1F)**. Extraction efficiency is ~10%, which is comparable to previously published results[6,11,12]. Compared to our previous, western blot-based assay, we observe significantly reduced signal in our negative controls. Importantly, the new assay retains physiological substrate selectivity as the mitochondrial TA protein Fis1 is not extracted in our assay **(Figure 1F)**. However, addition of a known Msp1 recognition sequence, the hydrophobic patch from Pex15, leads to robust Msp1-dependent extraction, consistent with previous results[6,16]. We conclude that the new assay has comparable extraction efficiency with our previously validated assay, but is faster, more quantitative, and has significantly improved signal to noise.

With a robust, quantitative, and physiological extraction assay now established, we next used this assay to examine the effects of the substrate TMD and lipid bilayer on Msp1 extraction activity. As proteoliposome reconstitutions are inherently variable, we took several steps to ensure experimental rigor and reproducibility. The extraction data involves at least 2 separate reconstitutions and between 2-4 technical replicates within each reconstitution. A new standard curve was generated for each new reconstitution. To ensure proper substrate reconstitution, a protease protection assay and a negative control (no ATP or ATPase deficient E193Q Msp1 mutant) was included in every assay.

Msp1 shows more robust extraction activity in thinner bilayers

An outstanding question in the field is how Msp1 recognizes substrates. Our data clearly demonstrates that the hydrophobic patch is sufficient for substrate recognition **(Figure 1F)**. However, the juxtamembrane hydrophobic patch is unique to Pex15 and does not appear to be widely conserved across other Msp1 substrates. We have previously proposed that Msp1 recognizes substrates by a hydrophobic mismatch between the TMD of the mislocalized substrate and the lipid bilayer[9].

To test this hypothesis, we first attempted to generate a hydrophobic mismatch by reconstituting the Sec22 model substrate into a series of liposomes composed of lipids with varying chain lengths. To minimize heterogeneity in the system, all liposomes were composed of phosphatidylcholine (PC) with both acyl chains containing a single cis double bond. The liposomes also contained 2% of DOGS-NiNTA, which was necessary to anchor soluble Msp1 to the liposomes. For simplicity, we will refer to the thickness liposomes as our T-series liposomes, with T1 referring to the thinnest liposomes (14:1, 14:1) and T5 the thickest liposomes (22:1, 22:1) **(Figure 2A)**.

DeepTMHMM predicts that the Sec22 model substrate has a TMD length of 20 amino acids[18]. Assuming a rise of 1.5 Å per residue in a standard α-helix, the Sec22 TMD is predicted to span 30 Å. Previous studies of liposomes composed of phosphatidyl choline with different acyl chain lengths demonstrated that each carbon in the acyl chain leads to an increase of 1.9 Å in the thickness of the hydrophobic core of a lipid bilayer[17] **(Figure 2A)**. This means that liposomes T1 and T2 with hydrophobic cores <31 Å are too thin to fully shield the TMD of Sec22, leading to a hydrophobic mismatch. Liposomes T3-T5 have hydrophobic cores > 32.6 Å

and can therefore easily accommodate the Sec22 TMD. Consistent with this model, the T1 and T2 liposomes show >35% extraction efficiency while substrate extraction drops < 20% for liposomes T3-T5 **(Figure 2B)**.

TMD residues are more exposed in thinner liposomes

To directly demonstrate increased exposure of TMD residues in a thinner lipid bilayer, we measured the solvent accessibility of a membrane-adjacent cysteine residue in our model substrate. We added a single cysteine residue to the N-terminus of the Sec22 TMD. We then reconstituted the substrate into our T-series liposomes and reacted the liposomes with PEG_{5000}-maleimide. If the cysteine residue is buried in the lipid bilayer, it will be protected from the membrane impermeable crosslinker. Conversely, a hydrophobic mismatch will lead to increased solvent exposure of the cysteine residue, resulting in increased labeling by PEG_{5000}-maleimide, which can be easily observed by a size shift on SDS PAGE. As a positive control, the liposomes were solubilized with 1% Triton X-100 during labeling. Consistent with the hydrophobic mismatch model, we see a clear decrease in cysteine labeling as the model substrate moves to thicker liposomes **(Figure 2D & E)**. We conclude that there is a strong positive correlation between hydrophobic mismatch of the substrate TMD with the lipid bilayer and Msp1 extraction activity.

Substrates with a longer TMD show enhanced extraction activity

A hydrophobic mismatch can be created either by using thinner lipid bilayers, as described above, or by increasing the length of TMD. The enhanced substrate extraction in the thinner bilayers could be due to either a hydrophobic mismatch between the substrate TMD and bilayer leading to enhanced substrate recognition or a lower thermodynamic barrier for substrate extraction leading to enhanced extraction kinetics[19]. Indeed, previous studies have shown that as the acyl chain length increases, the order of the lipid molecules increases[17]. Conversely, increasing the length of the TMD should increase the stability of the substrate in the lipid bilayer, thereby increasing the thermodynamic barrier for substrate extraction[20,21].

We therefore created a series of artificial substrates with TMD lengths ranging from 16-24 residues. To test the hypothesis that Msp1 recognizes a hydrophobic mismatch rather than specific sequences in the model substrate, we designed artificial TMDs composed solely of leucine and alanine residues[22] **(Figure 3A)**. To standardize the substrates, all TMDs were required to begin and end with leucine, have a GRAVY score of 3 +/- 0.2, and contain 10-13 leucine residues. We refer to these as our L-series substrates, with L16 having the shortest TMD at 16 residues and L24 having the longest TMD at 24 residues. The only difference between L-series substrates and the Sec22 model substrate is the TMD sequence and length.

We used an online calculator to predict the change in free energy for insertion of the L-series constructs into a model membrane[20,21] **(Figure 3A)**. As expected, TMD insertion into the bilayer was more favorable with a longer construct. The longer constructs should therefore have higher thermodynamic barriers for removal from the lipid bilayer and lower overall extraction. Conversely, the hydrophobic mismatch model predicts that the longer TMDs should lead to increased hydrophobic mismatch and therefore enhanced substrate extraction.

To distinguish between these two models, the L-series substrates were reconstituted into our standard liposomes and used in our extraction assay. All constructs showed ATP dependent extraction with L20, L22, and L24 showing higher extraction than L16, L18, and L19 **(Figure 3B)**. Assuming a rise of 1.5 Å per residue, constructs L16-L19 have TMD lengths < 30 Å and

therefore should not have a hydrophobic mismatch with our standard liposomes, which are predicted to a have hydrophobic core of 30-33 Å. By contrast, L20-L24 have TMD lengths of 30-36 Å and should have a hydrophobic mismatch.

While the change in extraction activity is relatively modest, it is significant and reproducible. As for any enzymatic process, catalytic efficiency depends on both substrate binding and the kinetics of the rate limiting step. As this is an end-point assay, care must be taken when interpreting the results as increased extraction activity could be due to either enhanced substrate recognition or faster kinetics at the rate limiting step. The simplest explanation for the modestly enhanced extraction of the L20-L24 constructs is that a hydrophobic mismatch leads to enhanced substrate recognition, which is partially counteracted by increased thermodynamic stability of the substrate in the lipid bilayer.

Variation of both substrate length and bilayer thickness supports hydrophobic mismatch model

Our standard liposomes contain a complex mixture of lipids which make it difficult to precisely predict the thickness of the hydrophobic core of the lipid bilayer. We also observed that too large of a discrepancy between TMD length and bilayer thickness led to low reconstitution efficiency. To gain full experimental control over the TMD length and bilayer thickness, we reconstituted the L-series substrates into the T-series liposomes.

We reconstituted the L20, L22, and L24 substrates into the T-series liposomes that most closely matched the predicted TMD length. For the L20 substrate, this involved reconstitution into T1, T2, and T3 liposomes. Based on the length of the L20 TMD and the thickness of the T-series liposomes, there should be a hydrophobic mismatch in T1, a possible mismatch in T2, and no mismatch in T3 liposomes. Consistent with this model, we observed the most robust extraction in T1 proteoliposomes and the weakest extraction in the T3 liposomes **(Figure 4A)**. Similar trends were observed with L22 in T2-T4 liposomes **(Figure 4C)** and L24 in T3 and T4 liposomes **(Figure 4E)**. We conclude that a hydrophobic mismatch between a substrate TMD and the lipid bilayer is a major driver of Msp1 substrate selectivity.

The rate limiting step in Msp1 activity is removal of the substrate from the lipid bilayer

Having firmly established that a hydrophobic mismatch between the substrate TMD and the lipid bilayer is the primary determinant of Msp1 extraction, we next sought to determine what is the rate limiting step in substrate extraction. It is currently unclear how substrates gain access to the Msp1 axial pore. Previous studies with soluble Msp1 working on soluble substrates concluded that Msp1 is a processive unfoldase that recognizes long, unstructured tails at the end of a substrate. This model predicts that Msp1 must first unfold cytosolic domains on a substrate before removing the TMD from the bilayer[23]. In such a model, there are two major thermodynamic barriers that could serve as the rate limiting step in the reaction, 1) unfolding of the cytosolic domain or 2) extraction of the TMD from the lipid bilayer.

To test if TMD removal from the lipid bilayer is the rate limiting step in substrate extraction, we reconstituted our standard Sec22 model substrate into liposomes with increasing levels of unsaturated acyl chains. If unfolding of the cytosolic domain is the rate limiting step in substrate extraction, then increasing the fluidity of the lipid bilayer should have no effect on substrate extraction. Conversely, if the rate limiting step is removal of the TMD from the bilayer, we expect to see enhanced extraction activity in the more fluid membrane.

To minimize heterogeneity in the system, all liposomes were composed of phosphatidylcholine with a chain length of 18 **(Figure 5A)**. For simplicity, we will refer to the

fluidity liposomes as our F-series liposomes, with F1 referring to the least fluid and F4 the most fluid. All liposomes were prepared in an identical manner and extruded through a 100 nm pore size. The molecular lipid packing densities were determined by using the fluorescent reporter C-Laurdan. The general polarization (GP) values followed the expected trend and were comparable to previously published values[24] **(Figure 5B)**.

We reconstituted our standard Sec22 model substrate into the F-series liposomes and observed a clear increase in substrate extraction with our most fluid liposomes **(Figure 5C)**. In principle, the enhanced extraction in the F4 liposomes could be due to either a lower thermodynamic barrier for removing the TMD from the lipid bilayer or increased exposure of the hydrophobic TMD residues in a more fluid bilayer. To distinguish between these models, we again turned to PEG_{5000}-maleimide labeling of our Sec22 substrate containing a single, TMD adjacent cysteine. Compared to the differences in cysteine reactivity observed in the T-series liposomes **(Figure 2D)**, we observed modest changes in cysteine reactivity between the F1 and F4 liposomes with no clear trend regarding membrane fluidity **(Figure 5E)**. We conclude that the differences in extraction activity most likely arise from a reduced thermodynamic barrier for removing a substrate from the lipid bilayer. Together, these results suggest that the rate limiting step in Msp1 activity is removal of the TMD from the lipid bilayer.

Discussion:

An essential aspect of membrane proteostasis is the removal of substrates from the membrane. However, our mechanistic understanding of this process, particularly the role of the lipid bilayer is incomplete. To address this knowledge gap, we developed a rapid and quantitative assay to measure Msp1-mediated substrate extraction from a lipid bilayer. We demonstrated that this assay has comparable extraction efficiency to our previously published assay, but with the added benefits of greater quantitation, faster turnaround time, and reduced background signal. Importantly, this system retains physiological substrate selectivity. Using this fully defined system, we systematically varied features of our model substrates and the lipid bilayer to understand the molecular basis for how Msp1 recognizes and removes substrates from the lipid bilayer. We demonstrated that Msp1 recognizes substrates through a hydrophobic mismatch between the substrate TMD and the lipid bilayer. Furthermore, we demonstrated that the rate limiting step in substrate extraction is removal of the TMD from the lipid bilayer rather than unfolding of the cytosolic domain.

<u>Msp1 recognizes substrates by a hydrophobic mismatch between the substrate TMD and the lipid bilayer</u>

Previous work had to led to the proposal of several different models for how Msp1 recognizes and extracts substrates. Weir et al. demonstrated that Msp1 extracts Pex15 from the peroxisome when it is in stoichiometric excess of its binding partner, Pex3[3]. This led to a model that orphaned substrates are less thermodynamically stable than a mature complex and/or expose an Msp1 recognition motif. However, subsequent studies demonstrated that Pex3 can directly inhibit Msp1 activity, casting doubt on this model[23]. Using a soluble Msp1 construct that was artificially hexamerized by fusion to the PAN N-domain, Castanzo et al. demonstrated that Msp1 recognizes long, unstructured polypeptides[23]. However, the rate of substrate processing was quite slow, with a V_{Max} of 0.1 substrates $hexamer^{-1}$ min^{-1}. It should also be noted that these studies used fully soluble (ΔTMD) Msp1 and substrates, so the physiological significance is unclear.

Both of these models suggest that substrate thermodynamic stability plays a major role in regulating Msp1 activity.

Li et al. used photo-crosslinking to demonstrate that a juxtamembrane hydrophobic patch is critical for Msp1-Pex15 interactions[16]. Addition of this hydrophobic patch to the mitochondrial TA protein Fis1 is sufficient to convert it into an Msp1 substrate. This is a particularly appealing model as recent cryo-EM structures of *C. thermophilum* Msp1 and human ATAD1 show an exposed hydrophobic pocket within the N-domain that could provide a membrane adjacent binding site for such a hydrophobic patch[25,26]. However, few Msp1 substrates contain similar hydrophobic patches, raising questions about the generality of a hydrophobic patch.

We propose that a hydrophobic mismatch between the substrate TMD and the lipid bilayer is the predominant mechanism for Msp1 substrate interactions. This model is particularly enticing as the predominant substrate for Msp1, mislocalized ER-TA, are likely to exhibit a hydrophobic mismatch. Previous work has established that ER-TA proteins tend to be longer and more hydrophobic than mitochondrial TA proteins[27]. Furthermore, ER membranes tend to be slightly thicker than the OMM. Therefore, mislocalized ER-TA proteins will likely have a hydrophobic mismatch with the OMM, leading to exposed hydrophobic residues that will drive Msp1 engagement[27].

Model for Msp1 mediated substrate extraction

If the hydrophobic mismatch is the predominant means of substrate recognition, then Msp1 is likely engaging with the middle of the substrate rather than the terminus. This raises the question of how a membrane anchored substrate can gain access to the axial pore of the membrane anchored Msp1 ring. We can envision two potential models that overcome this geometric problem. First, a substrate could laterally diffuse into the axial pore through a gap in the Msp1 ring. Second, the Msp1 ring could assemble around a substrate. The ring assembly model is supported by biochemical data showing that WT Msp1 does not form a constitutive hexamer *in vitro* or *in vivo*. The lateral diffusion model is supported by cryo-EM structures of ATPase inactive Msp1 hexamers in a lock-washer conformation with a seam that could support lateral diffusion of the substrate into the axial pore[25,26]. A particularly attractive feature of this model is that the cryo-EM structure of Msp1 shows an exposed hydrophobic groove in the N-domain of the Msp1 subunit the forms part of the seam in the lock washer. As the N-domain is exposed to the lipid bilayer, this provides an obvious mechanism for simultaneously recognizing a hydrophobic mismatch and facilitating lateral diffusion of the substrate into the axial pore. Further experiments are needed to distinguish between these models.

While our results demonstrate a prominent role for a hydrophobic mismatch in substrate recognition, they do not exclude the possibility of processive substrate unfolding driven by the Msp1 pore loops directly engaging with long, unstructured regions on the substrate terminus. Indeed, many AAA+ proteins have bipartite substrate recognition motifs, with long-unstructured regions showing non-sequence specific engagement with the pore loops.

In conclusion, we have developed a new assay to monitor the extraction of membrane proteins from a lipid bilayer by the AAA+ motor protein Msp1. Using this fully defined system, we systematically probed the role of the membrane composition and substrate TMD of Msp1 activity. We discovered that Msp1 recognizes substrates by a hydrophobic mismatch between the substrate TMD and the lipid bilayer. We also demonstrated that the rate limiting step in substrate extraction is removal of the TMD from the lipid bilayer.

Materials and Methods:

Soluble Protein Purification

Δ1-32 Msp1

Plasmids were transformed into *E. coli* BL21(DE3) containing a pRIL plasmid and expressed in terrific broth at 37°C until an OD600 of 0.6–1.0, cultures were induced with 0.25 mM IPTG and grown at room temperature for an additional 3–4 hr. Cells were harvested by centrifugation, and resuspended in Msp1 Lysis Buffer (20 mM Tris pH 7.5, 200 mM KAc, 20 mM imidazole, 0.01 mM EDTA, 1 mM DTT) supplemented with 0.05 mg/mL lysozyme (Sigma), 1 mM phenylmethanesulfonyl fluoride (PMSF) and 500 U of universal nuclease (Pierce), and lysed by sonication. The supernatant was isolated by centrifugation for 30 min at 4°C at 18,500 × *g* and purified by Ni-NTA affinity chromatography (Pierce) on a gravity column. Ni-NTA resin was washed with 10 column volumes (CV) of Msp1 Lysis Buffer and then 10 CV of Wash Buffer (Msp1 Lysis buffer with 30 mM imidazole) before elution with Lysis Buffer supplemented with 250 mM imidazole.

The protein was further purified by size exclusion chromatography (SEC) (Superdex 200 Increase 10/300 GL, GE Healthcare) in 20 mM Tris pH 7.5, 200 mM KAc, 1 mM DTT. Peak fractions were pooled, concentrated to 5–15 mg/mL in a 30 kDa MWCO Amicon Ultra centrifugal filter (Pierce) and aliquots were flash-frozen in liquid nitrogen and stored at –80°C. Protein concentrations were determined by A280 using a calculated extinction coefficient (Expasy).

SGTA and Calmodulin

GST-SGTA and GST-calmodulin were expressed as described above for soluble Msp1 constructs. Cells were harvested by centrifugation and resuspended in SGTA Lysis Buffer (50 mM HEPES pH 7.5, 150 mM NaCl, 0.01 mM EDTA, 1 mM DTT, 10% glycerol) supplemented with 0.05 mg/mL lysozyme (Sigma), 1 mM PMSF and 500 U of universal nuclease (Pierce), and lysed by sonication. The supernatant was isolated by centrifugation for 30 min at 4°C at 18,500 × *g* and purified by glutathione affinity chromatography (Thermo Fisher) on a gravity column. Resin was washed with 20 CV of SGTA Lysis Buffer and then eluted with 3 CV of SGTA Lysis Buffer supplemented with 10 mM reduced glutathione. The protein was further purified by SEC (Superdex 200 Increase 10/300 GL, GE Healthcare) in 20 mM Tris pH 7.5, 100 mM NaCl, 0.1 mM TCEP. Peak fractions were pooled, concentrated to 10 mg/mL in a 30 kDa MWCO Spin Concentrator (Pierce) and aliquots were flash-frozen in liquid nitrogen and stored at –80°C. Protein concentrations were determined by A280 using a calculated extinction coefficient (Expasy).

LgBiT and MBP-Ubiquitin

LgBiT and MBP-Ubiquitin were expressed as described above for soluble Msp1 constructs. Cells were harvested by centrifugation and resuspended in Lysis Buffer (20 Tris 7.5, 200 NaCl, 1 DTT, 0.01 EDTA, 20 mM imidazole) supplemented with 0.05 mg/mL lysozyme (Sigma), 1 mM PMSF and 500 U of universal nuclease (Pierce), and lysed by sonication. The supernatant was isolated by centrifugation for 30 min at 4°C at 18,500 × *g* and purified by Ni-NTA affinity chromatography (Pierce) on a gravity column. Ni-NTA resin was washed with 10 column volumes (CV) of Msp1 Lysis Buffer and then 10 CV of Wash Buffer (20 Tris 7.5, 200 NaCl, 1 DTT, 0.01 EDTA, 30 mM imidazole) before elution with Lysis Buffer supplemented with 250 mM imidazole. The protein was further purified by size exclusion chromatography (SEC)

(Superdex 200 Increase 10/300 GL, GE Healthcare) in 20 mM Tris pH 7.5, 200 mM NaCl, 1 mM DTT. Peak fractions were pooled, concentrated to 5–15 mg/mL in a 30 kDa MWCO Amicon Ultra centrifugal filter (Pierce) and aliquots were flash-frozen in liquid nitrogen and stored at –80°C. Protein concentrations were determined by A280 using a calculated extinction coefficient (Expasy).

Membrane Protein Purification

SumoTMD substrates

The main substrate (SUMO-Sec22 TMD) is in a pET28a plasmid backbone. Cloning of all synthetic TMD substrates was conducted via traditional PCR/restriction enzyme 'cut and paste' methods to swap out Sec22 TMD and verified by Sanger sequencing. The layout of all constructs is His_6-3C protease site-3xFlag-SUMO-*TMD*-thrombin protease site-HiBiT tag. After transforming the SumoTMD plasmid into *E. coli* BL21(DE3)/pRIL, the cells were grown in terrific broth at 37°C until an OD_{600} of 0.6-0.8, and then induced with 0.25 mM IPTG and grown at room temperature for an additional 3-4 hr. Cells were harvested by centrifugation, and resuspended in SumoTMD Lysis Buffer (50 mM Tris pH 7.5, 300 mM NaCl, 10 mM $MgCl_2$, 10 mM Imidazole, 10% glycerol) supplemented with 0.05 mg/mL lysozyme (Sigma), 1 mM PMSF and 500 U of benzonase (Sigma), and lysed by sonication. Membrane proteins were solubilized by addition of n-dodecyl-β-D-maltoside (DDM) to a final concentration of 1% and rocked at 4°C for 30'. Lysate was cleared by centrifugation at 4°C for 1 hr at 35,000 x g and purified by Ni-NTA affinity chromatography.

Ni-NTA resin was washed with 10 column volumes (CV) of SumoTMD Wash Buffer 1 (50 mM Tris pH 7.5, 500 mM NaCl, 10 mM $MgCl_2$, 10 mM imidazole, 5 mM β-mercaptoethanol (BME), 10% glycerol, 0.1% DDM). Resin was then washed with 10 CV of SumoTMD Wash Buffer 2 (same as Wash Buffer 1 except with 300 mM NaCl and 25 mM imidazole) and 10 CV of SumoTMD Wash Buffer 3 (same as Wash Buffer 1 with 150 mM NaCl and 50 mM imidazole) and then eluted with 3 CV of SumoTMD Elution Buffer (same as Wash Buffer 3 except with 250 mM imidazole).

The protein was further purified by size exclusion chromatography (SEC) (Superdex 200 Increase 10/300 GL, GE Healthcare) in 50 mM Tris pH 7.5, 150 mM NaCl, 10 mM $MgCl_2$, 5 mM BME, 10% glycerol, 0.1% DDM. Peak fractions were pooled, aliquots were flash-frozen in liquid nitrogen and stored at –80°C. Protein concentrations were determined by A_{280} using a calculated extinction coefficient (Expasy).

Liposome preparation

Liposomes mimicking the lipid composition of the yeast OMM, as well as the thickness and fluidity series, were prepared as described previously[7]. Briefly, a lipid film was prepared by mixing chloroform stocks of lipids applicable to each type of liposome as shown below. Chloroform was evaporated under a gentle steam of nitrogen and then left on a vacuum (<1 mTorr) overnight. Lipid film was fully resuspended in Liposome Buffer (50 mM HEPES KOH pH 7.5, 15% glycerol, 1 mM DTT) to a final concentration of 20 mg/mL and then subjected to five freeze-thaw cycles with liquid nitrogen. Liposomes were extruded 15 times through a 100 nm filter at 60°C, distributed into single-use aliquots, and flash-frozen in liquid nitrogen.

Nickel liposomes

Chicken egg phosphatidyl choline (Avanti 840051C), chicken egg phosphatidyl ethanolamine (Avanti 840021C), bovine liver phosphatidyl inositol (Avanti 840042C), synthetic DOPS (Avanti 840035C), synthetic TOCL (Avanti 710335C), and 1,2-dioleoyl-*sn*-glycero-3-[*N*-((5-amino-1-carboxypentyl)iminodiacetic acid)succinyl] Nickel salt (Avanti 790404) at a 48:28:10:8:4:2 molar ratio with 1 mg of DTT.

T-series liposomes
T1: synthetic 14:1, 14:1 phosphatidyl choline (Avanti 850346C) and synthetic 18:1, 18:1 1,2-dioleoyl-*sn*-glycero-3-[*N*-((5-amino-1-carboxypentyl)iminodiacetic acid)succinyl] Nickel salt (Avanti 790404) at a 98:2 molar ratio with 1 mg of DTT.
T2: synthetic 16:1, 16:1 phosphatidyl choline (Avanti 850358C) and synthetic 18:1, 18:1 1,2-dioleoyl-*sn*-glycero-3-[*N*-((5-amino-1-carboxypentyl)iminodiacetic acid)succinyl] Nickel salt (Avanti 790404) at a 98:2 molar ratio with 1 mg of DTT.
T3: synthetic 18:1, 18:1 phosphatidyl choline (Avanti 850375C) and synthetic 18:1, 18:1 1,2-dioleoyl-*sn*-glycero-3-[*N*-((5-amino-1-carboxypentyl)iminodiacetic acid)succinyl] Nickel salt (Avanti 790404) at a 98:2 molar ratio with 1 mg of DTT.
T4: synthetic 20:1, 20:1 phosphatidyl choline (Avanti 850396C) and synthetic 18:1, 18:1 1,2-dioleoyl-*sn*-glycero-3-[*N*-((5-amino-1-carboxypentyl)iminodiacetic acid)succinyl] Nickel salt (Avanti 790404) at a 98:2 molar ratio with 1 mg of DTT.
T5: synthetic 22:1, 22:1 phosphatidyl choline (Avanti 850398C) and synthetic 18:1, 18:1 1,2-dioleoyl-*sn*-glycero-3-[*N*-((5-amino-1-carboxypentyl)iminodiacetic acid)succinyl] Nickel salt (Avanti 790404) at a 98:2 molar ratio with 1 mg of DTT.

F-series liposomes
F1: synthetic 18:1, 18:1, *trans* phosphatidyl choline (Avanti 850376C) and synthetic 18:1, 18:1 1,2-dioleoyl-*sn*-glycero-3-[*N*-((5-amino-1-carboxypentyl)iminodiacetic acid)succinyl] Nickel salt (Avanti 790404) at a 98:2 molar ratio with 1 mg of DTT.
F2: synthetic 18:0, 18:1 phosphatidyl choline (Avanti 850467C) and synthetic 18:1, 18:1 1,2-dioleoyl-*sn*-glycero-3-[*N*-((5-amino-1-carboxypentyl)iminodiacetic acid)succinyl] Nickel salt (Avanti 790404) at a 98:2 molar ratio with 1 mg of DTT.
F3: synthetic 18:1, 18:1, *cis* phosphatidyl choline (Avanti 850375C) and synthetic 18:1, 18:1 1,2-dioleoyl-*sn*-glycero-3-[*N*-((5-amino-1-carboxypentyl)iminodiacetic acid)succinyl] Nickel salt (Avanti 790404) at a 98:2 molar ratio with 1 mg of DTT.
F4: synthetic 18:2, 18:2 phosphatidyl choline (Avanti 850385C) and synthetic 18:1, 18:1 1,2-dioleoyl-*sn*-glycero-3-[*N*-((5-amino-1-carboxypentyl)iminodiacetic acid)succinyl] Nickel salt (Avanti 790404) at a 98:2 molar ratio with 1 mg of DTT.

Reconstitution into Liposomes
For extraction assays proteoliposomes were prepared by mixing 2 μM TA protein (SumoTMD), and 2 mg/mL of Nickel liposomes in Reconstitution Buffer. Detergent was removed by adding 25 mg of biobeads and rotating the samples for 16 hr at 4°C. Material was removed from biobeads and added to fresh 25 mg biobeads and rotated for another 1-3 hr at RT. Unincorporated TA protein was pre-cleared by incubating the reconstituted material with excess (5 μM) GST-SGTA and GST-calmodulin and passing over a glutathione spin column (Pierce #16103); the flow through was collected and used immediately for dislocation assays.

C-Laurdan Spectroscopy

C-laurdan spectroscopy was performed by using 10 µL of pre-formed F-series liposomes and 90 µl of extraction buffer (50 mM Hepes pH 7.5, 200 mM KAc, 7 mM MgAc, 2 mM DTT, 10 µm Ca^{2+}) to match overnight reconstitution volume. Final 50 µg/ml of C-laurdan dye (Fisher) was added and a fluorescence spectrum was read. The sample was excited at 375 nm and an emission spectrum from 400 to 600 nm with 3 nm step size was recorded. The GP value (-1 most disordered, +1 most ordered membranes) was measured as described previously[28] by integrating the intensities between 400 and 460 nm (I_{Ch1}), and 470 and 530 nm (I_{Ch2}):

$GP = (I_{CH1} - I_{CH2}) / (I_{CH1} + I_{CH2})$.

Extraction Assay

Extraction assays contained 30 µL of pre-cleared proteoliposomes, 5 µM GST-SGTA, 5 µM GST-calmodulin, 3 µM Msp1, 8 µM MBP-Ubiquitin, 1 mg/mL bovine serum albumin (sigma), and 110 mM ATP and the final volume was adjusted to 100 µL with Extraction Buffer (50 mM HEPES KOH pH 7.5, 200 mM potassium acetate, 7 mM magnesium acetate, 2 mM DTT, 0.1 µM calcium chloride). Samples were incubated at 30°C for 30 minutes and then transferred to ice. Samples were transferred to polycarbonate centrifuge tubes (Beckman-Coulter #343776) and centrifuged at 150,000 x *g* in TLA-120.1 Fixed-Angle Rotor (Beckman-Coulter) for 30' at 4˚C. The top 20 ul was collected and combined with 1.5 µM LgBiT and the final volume was adjusted to 50 µL with Extraction Buffer. After incubating at RT for 25 minutes, samples were plated onto white 96-well plates (Corning #07201204) and 20 µL of lytic furimazine (Promega #N3030) was added. Immediately plates were read at 480 nm wavelength to measure luminescence.

Standard curve measurements

Standards were made starting with 20% of the volume of pre-cleared liposomes used in the extraction and brought up to 100 µL with Extraction Buffer (50 mM HEPES KOH pH 7.5, 200 mM potassium acetate, 7 mM magnesium acetate, 2 mM DTT, 0.1 µM calcium chloride). This was then diluted to make 15%, 10%, and 5% samples. 20 µL from each was then combined with 1.5 µM LgBiT and the final volume was adjusted to 50 µL with Extraction Buffer. After incubating at RT for 25 minutes, samples were plated onto white 96-well plates (Corning #07201204) and 20 µL of lytic furimazine (Promega #N3030) was added. Immediately plates were read at 480 nm wavelength to measure luminescence.

Protease Protection Assay

Protease protection assay was carried out in a 10 µL total volume with 7 µL of pre-cleared liposomes, 2 U of thrombin protease, and 1% of Triton X-100 (where indicated). Samples were incubated at RT for 1 hour and then 1 µL of 200 mM PMSF was added. The samples were reverse quenched into 90 µL of boiling 1% SDS and incubated at 95˚C for 10 minutes. Anti-HiBiT western blot was then performed with 1:5,000 dilution of mouse anti-HiBit (Promega, Clone 30E5) and 1:10,000 dilution of goat anti-mouse-HRP secondary antibody (Invitrogen).

PEG-Maleimide Assay

PEG maleimide labeling assay was carried out in a 10 µL total volume with 2 µL of pre-cleared material, and a 16 mM final concentration of methoxy PEG_{5000}-maleimide (JenKem). Reaction was incubated on ice for 30' and then quenched by the addition of DTT to a final concentration

of 100 mM. Sample was diluted by mixing with 90 µL of 1% SDS. SDS PAGE Loading Buffer was then added to a final concentration of 1x and samples were boiled for 20 minutes. Anti-HiBiT western blot was then performed with 1:5,000 dilution of mouse anti-HiBit (Promega, Clone 30E5) and 1:10,000 dilution of goat anti-mouse-HRP secondary antibody (Invitrogen).

Acknowledgements
The authors wish to thank members of the Wohlever lab for helpful discussions and feedback on the project.
Funding: This work was supported by NIH grant R35GM137904 (MLW).
Author Contributions: Conceptualization: HLF, MLW; Methodology: HLF, DG, MLW; Investigation: HLF, DG; Writing – Original Draft: HLF, MLW; Writing – Review and Editing: HLF, DG, MLW; Supervision and Funding Acquisition: MLW
Competing Interests: The authors declare no competing interests.

References:

1. Okreglak, V. & Walter, P. The conserved AAA-ATPase Msp1 confers organelle specificity to tail-anchored proteins. *Proceedings of the National Academy of Sciences* 111, 8019–8024 (2014).

2. Chen, Y.-C. *et al.* Msp1/ATAD1 maintains mitochondrial function by facilitating the degradation of mislocalized tail-anchored proteins. *The EMBO journal* 33, 1548–1564 (2014).

3. Weir, N. R., Kamber, R. A., Martenson, J. S. & Denic, V. The AAA protein Msp1 mediates clearance of excess tail-anchored proteins from the peroxisomal membrane. *eLife* 6, e28507 (2017).

4. Weidberg, H. & Amon, A. MitoCPR – a surveillance pathway that protects mitochondria in response to protein import stress. *Science (New York, NY)* 360, (2018).

5. Zhang, J. *et al.* The AAA+ ATPase Thorase regulates AMPA receptor-dependent synaptic plasticity and behavior. *Cell* 145, 284–299 (2011).

6. Winter, J. M. *et al.* Collateral deletion of the mitochondrial AAA+ ATPase ATAD1 sensitizes cancer cells to proteasome dysfunction. *Elife* 11, e82860 (2022).

7. Ahrens-Nicklas, R. C. *et al.* Precision therapy for a new disorder of AMPA receptor recycling due to mutations in ATAD1. *Neurology Genetics* 3, e130-11 (2017).

8. Umanah, G. K. E. *et al.* Thorase variants are associated with defects in glutamatergic neurotransmission that can be rescued by Perampanel. *Science translational medicine* 9, eaah4985 (2017).

9. Fresenius, H. L. & Wohlever, M. L. Sorting out how Msp1 maintains mitochondrial membrane proteostasis. *Mitochondrion* 49, 128–134 (2019).

10. Wang, L. & Walter, P. Msp1/ATAD1 in Protein Quality Control and Regulation of Synaptic Activities. *Annu Rev Cell Dev Bi* 36, 1–24 (2020).

11. Fresenius, H. L. & Wohlever, M. L. Reconstitution of Msp1 Extraction Activity with Fully Purified Components. *J Vis Exp* (2021) doi:10.3791/62928.

12. Wohlever, M. L., Mateja, A., McGilvray, P. T., Day, K. J. & Keenan, R. J. Msp1 Is a Membrane Protein Dislocase for Tail-Anchored Proteins. *Molecular Cell* 67, 194-202.e6 (2017).

13. England, C. G., Ehlerding, E. B. & Cai, W. NanoLuc: A Small Luciferase Is Brightening Up the Field of Bioluminescence. *Bioconjugate Chem* 27, 1175–1187 (2016).

14. Hall, M. P. *et al.* Engineered Luciferase Reporter from a Deep Sea Shrimp Utilizing a Novel Imidazopyrazinone Substrate. *Acs Chem Biol* 7, 1848–1857 (2012).

15. Leshchiner, E. S., Braun, C. R., Bird, G. H. & Walensky, L. D. Direct activation of full-length proapoptotic BAK. *Proceedings of the National Academy of Sciences of the United States of America* 110, E986–E995 (2013).

16. Li, L., Zheng, J., Wu, X. & Jiang, H. Mitochondrial AAA-ATPase Msp1 detects mislocalized tail-anchored proteins through a dual-recognition mechanism. *Embo Rep* 20, (2019).

17. Lee, T.-H., Sani, M.-A., Overall, S., Separovic, F. & Aguilar, M.-I. Effect of phosphatidylcholine bilayer thickness and molecular order on the binding of the antimicrobial peptide maculatin 1.1. *Biochimica Et Biophysica Acta Bba - Biomembr* 1860, 300–309 (2018).

18. Hallgren, J. *et al.* DeepTMHMM predicts alpha and beta transmembrane proteins using deep neural networks. (2022) doi:10.1101/2022.04.08.487609.

19. Guerriero, C. J. *et al.* Transmembrane helix hydrophobicity is an energetic barrier during the retrotranslocation of integral membrane ERAD substrates. *Molecular biology of the cell* 28, 2076–2090 (2017).

20. Hessa, T. *et al.* Molecular code for transmembrane-helix recognition by the Sec61 translocon. *Nature* 450, 1026–1030 (2007).

21. Hessa, T. *et al.* Recognition of transmembrane helices by the endoplasmic reticulum translocon. *Nature* 433, 377–381 (2005).

22. Fry, M. Y., Saladi, S. M. & Clemons, W. M. The STI1-domain is a flexible alpha-helical fold with a hydrophobic groove. *Protein Sci* 30, 882–898 (2021).

23. Castanzo, D. T., LaFrance, B. & Martin, A. The AAA+ ATPase Msp1 is a processive protein translocase with robust unfoldase activity. *Proc National Acad Sci* 117, 14970–14977 (2020).

24. Halbleib, K. *et al.* Activation of the Unfolded Protein Response by Lipid Bilayer Stress. *MOLCEL* 67, 673-684.e8 (2017).

25. Wang, L., Toutkoushian, H., Belyy, V., Kokontis, C. Y. & Walter, P. Conserved structural elements specialize ATAD1 as a membrane protein extraction machine. *Elife* 11, (2022).

26. Wang, L., Myasnikov, A., Pan, X. & Walter, P. Structure of the AAA protein Msp1 reveals mechanism of mislocalized membrane protein extraction. *eLife* 9, (2020).

27. Rao, M. *et al.* Multiple selection filters ensure accurate tail-anchored membrane protein targeting. *eLife* (2016) doi:10.7554/elife.21301.001.

28. Ballweg, S. *et al.* Regulation of lipid saturation without sensing membrane fluidity. *Nat Commun* 11, 756 (2020).

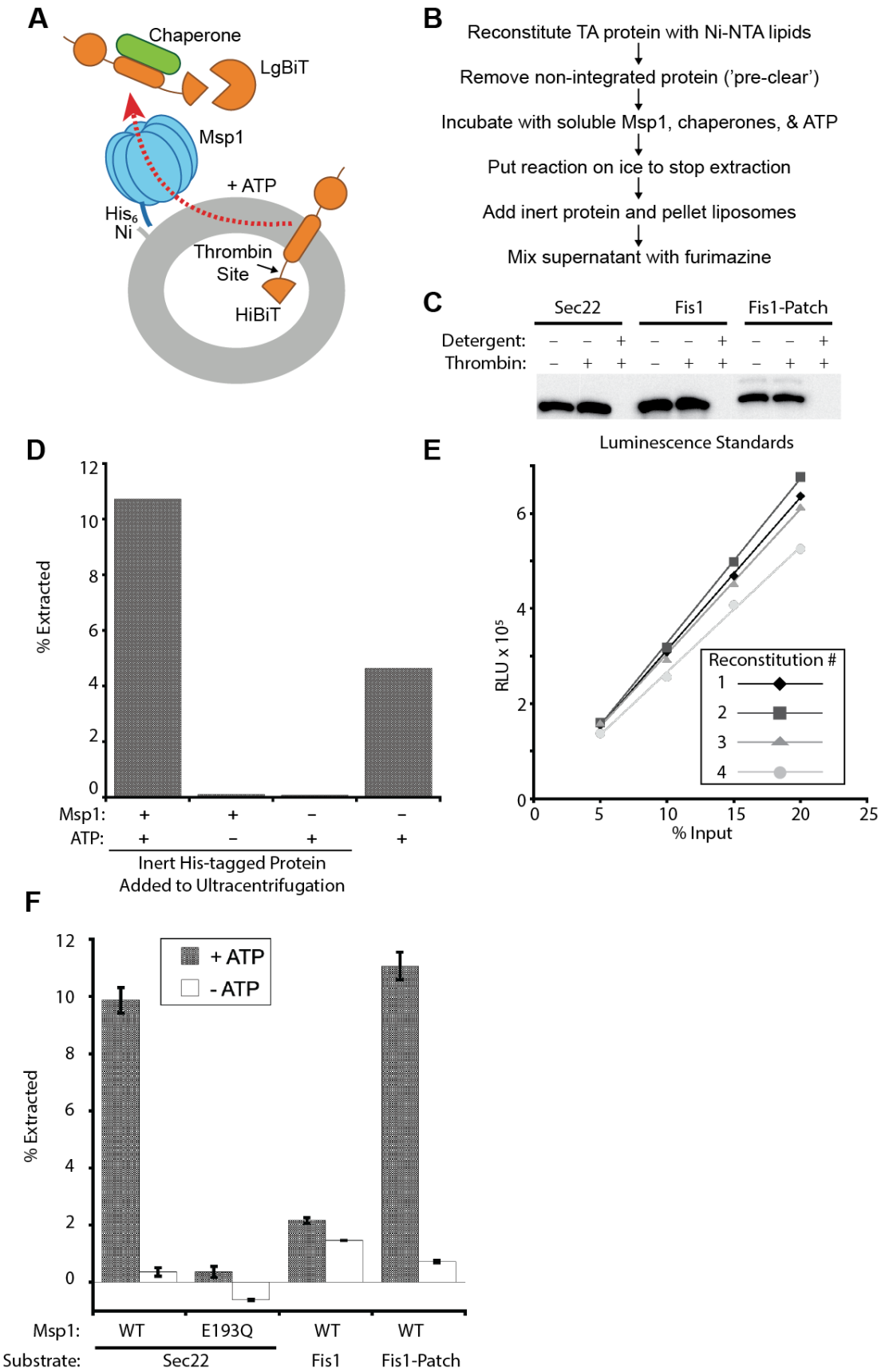
A
Chaperone
LgBiT
Msp1
+ ATP
His6
Ni
Thrombin
Site
HiBiT
B
Reconstitute TA protein with Ni-NTA lipids
Remove non-integrated protein ('pre-clear')
Incubate with soluble Msp1, chaperones, & ATP
Put reaction on ice to stop extraction
Add inert protein and pellet liposomes
Mix supernatant with furimazine
C
Sec22
Fis1
Fis1-Patch
Detergent:
Thrombin:
D
% Extracted
Msp1:
ATP:
Inert His-tagged Protein
Added to Ultracentrifugation
E
Luminescence Standards
RLU x 10^5
% Input
Reconstitution #
1
2
3
4
F
+ ATP
- ATP
% Extracted
Msp1:
Substrate:
WT
E193Q
WT
WT
Sec22
Fis1
Fis1-Patch

Figure 1: Validation of the split-luciferase based extraction assay

A) Diagram for split-luciferase extraction assay. Note that for properly reconstituted liposomes, both the HiBiT and thrombin sites are in the lumen of the proteoliposome.

B) Workflow for split-luciferase assay.

C) Protease protection assay shows that substrates are properly oriented. Anti-HiBiT western blot of pre-cleared liposomes shows minimal loss of signal upon addition of thrombin protease, but complete loss of signal with both thrombin and detergent.

D) Addition of an inert His_6-tagged protein to ultracentrifugation improves liposome pelleting efficiency and reduces background activity.

E) Standard curves used to calculate percent substrate extracted. Four separate reconstitutions of the standard Sumo-Sec22 model substrate in standard liposomes show a linear and reproducible signal. Different concentrations of pre-cleared, but unreacted proteoliposomes were mixed with LgBiT and furimazine reagent in detergent, which permeablizes the proteoliposomes. The X-axis refers to the percent of pre-cleared liposomes in the extraction assay.

F) The split-luciferase extraction assay shows ATP-dependent and physiological substrate extraction activity. The known substrate Sec22 extracted whereas the native mitochondrial protein Fis1 is not extracted unless a hydrophobic patch is added, which serves as an Msp1 recognition sequence. Error bars show standard error of the mean.

A

Liposome	Lipid	Measured Thickness (Å)	Fit Thickness (Å)
T1	PC (14:1, 14:1)	27.7	26.6
T2	PC (16:1, 16:1)	30.9	30.4
T3	PC (18:1, 18:1)	32.6	34.2
T4	PC (20:1, 20:1)	38	38
T5	PC (22:1, 22:1)	41.8	43

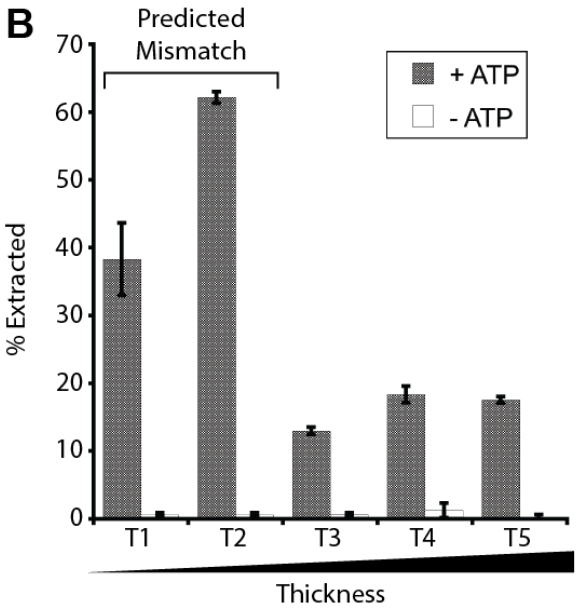

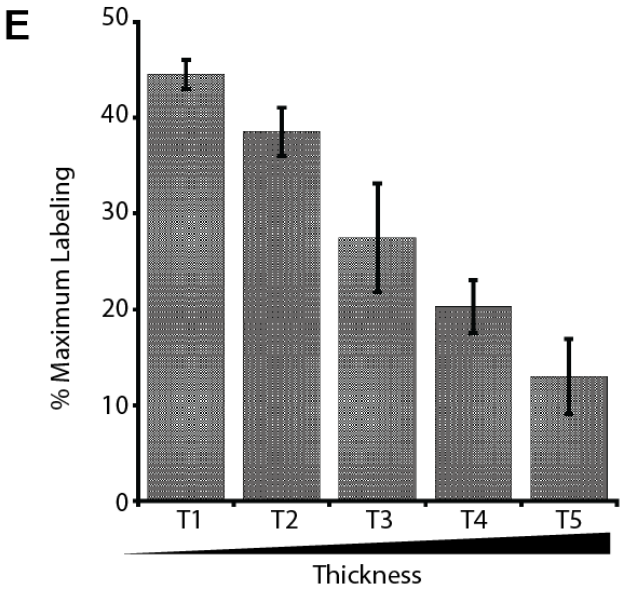

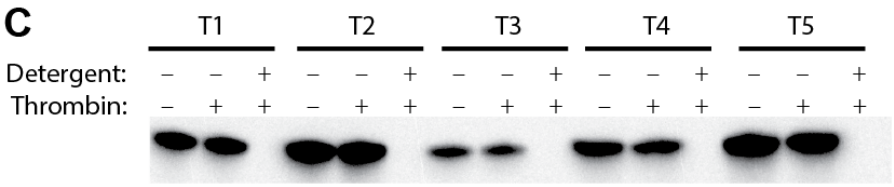

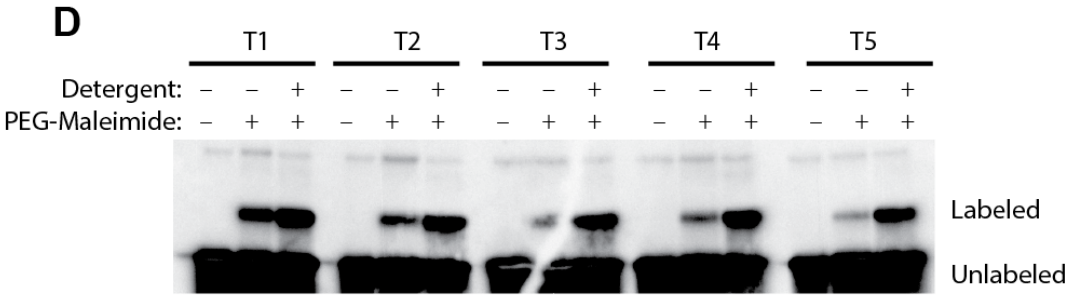

Figure 2: Msp1 shows more robust extraction activity in thinner bilayers

A) Composition and thickness of T-series liposomes. Values in the "measured thickness" column show previously measured values for the thickness of the hydrophobic core of phosphatidyl choline lipid bilayers[17]. In that same study, the authors demonstrated that the thickness of the hydrophobic core of a lipid bilayer could be calculated using the formula of 1.9 Å per carbon in the acyl chain. These calculated values are shown in the "fit thickness" column.

B) Msp1 shows more robust extraction activity in thinner liposomes. Extraction of the standard Sumo-Sec22 substrate in T-series liposomes. There is a predicted hydrophobic mismatch in T1 and T2 liposomes.

C) Protease protection assay of standard Sumo-Sec22 substrate in T-series liposomes. Anti-HiBiT western blot.

D) PEG-maleimide labeling shows increased TMD exposure in thinner liposomes. Anti-HiBiT western blot.

E) Quantification of data from **D** from 3 separate reconstitutions. Error bars show standard error of the mean. The amount of labeled material in the "+ detergent, + PEG-maleimide" lane is defined as 100% labeling.

A

Construct	Length (Å)	GRAVY	G Insertion (kCal/mol)	Sequence
L16	24	3.05	-2.29	LALLALLALLALALAL
L18	27	3.17	-3.31	LLALALLALLALAALLAL
L19	28.5	3.17	-4.39	LLLALALLALLALALLALL
L20	30	3.00	-4.23	LLALALLAALLALLALAALL
L22	33	2.89	-4.60	LLLAALALAALALLALALAALL
L24	36	2.8	-4.91	LLALAALALAALALALALALAALL

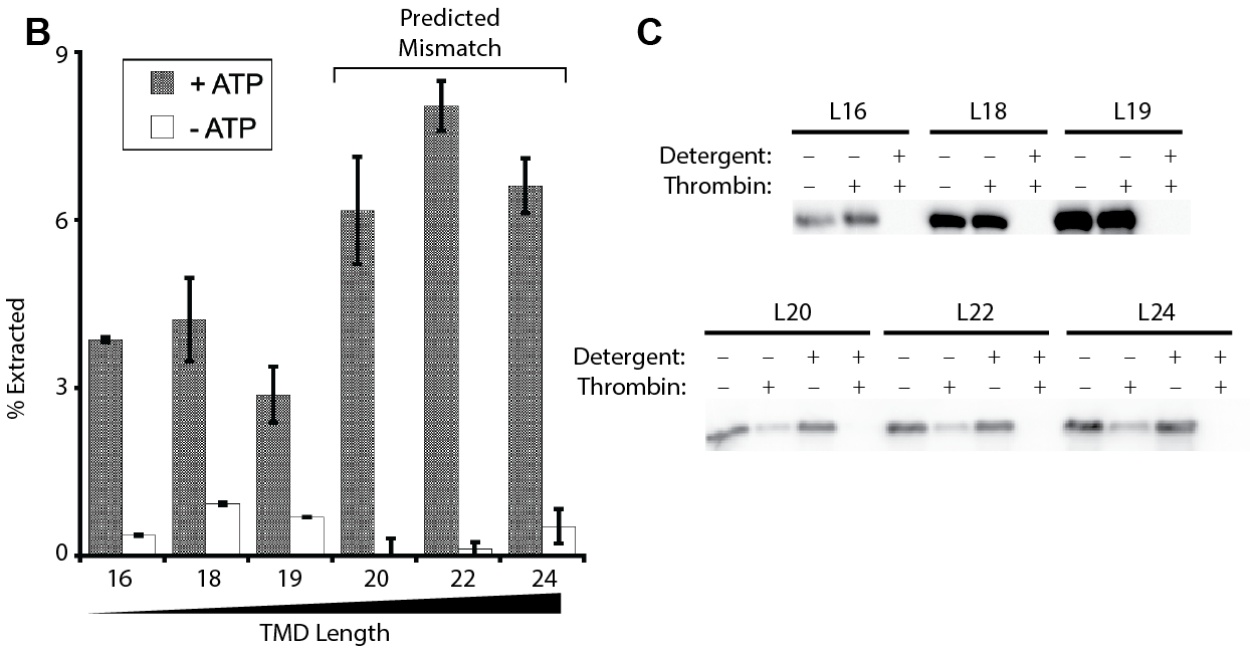

Figure 3: Design and extraction of L-Series Substrates bilayers

A) Design of L-series substrates. The length of the TMD is calculated by assuming a rise of 1.5 Å per residue. GRAVY score was calculated by inserting the TMD sequence into the GRAVY calculator (https://www.gravy-calculator.de/). The ΔG for TMD insertion was calculated using the website (https://dgpred.cbr.su.se/index.php?p=TMpred)[20,21]. TMD sequences for L-series substrates all start and end with Leucine.

B) L-series substrates with a predicted hydrophobic mismatch show enhanced extraction activity. L-series substrates were reconstituted in standard liposomes.

C) Protease protection assay of L-series substrates in standard liposomes. Anti-HiBiT western blot.

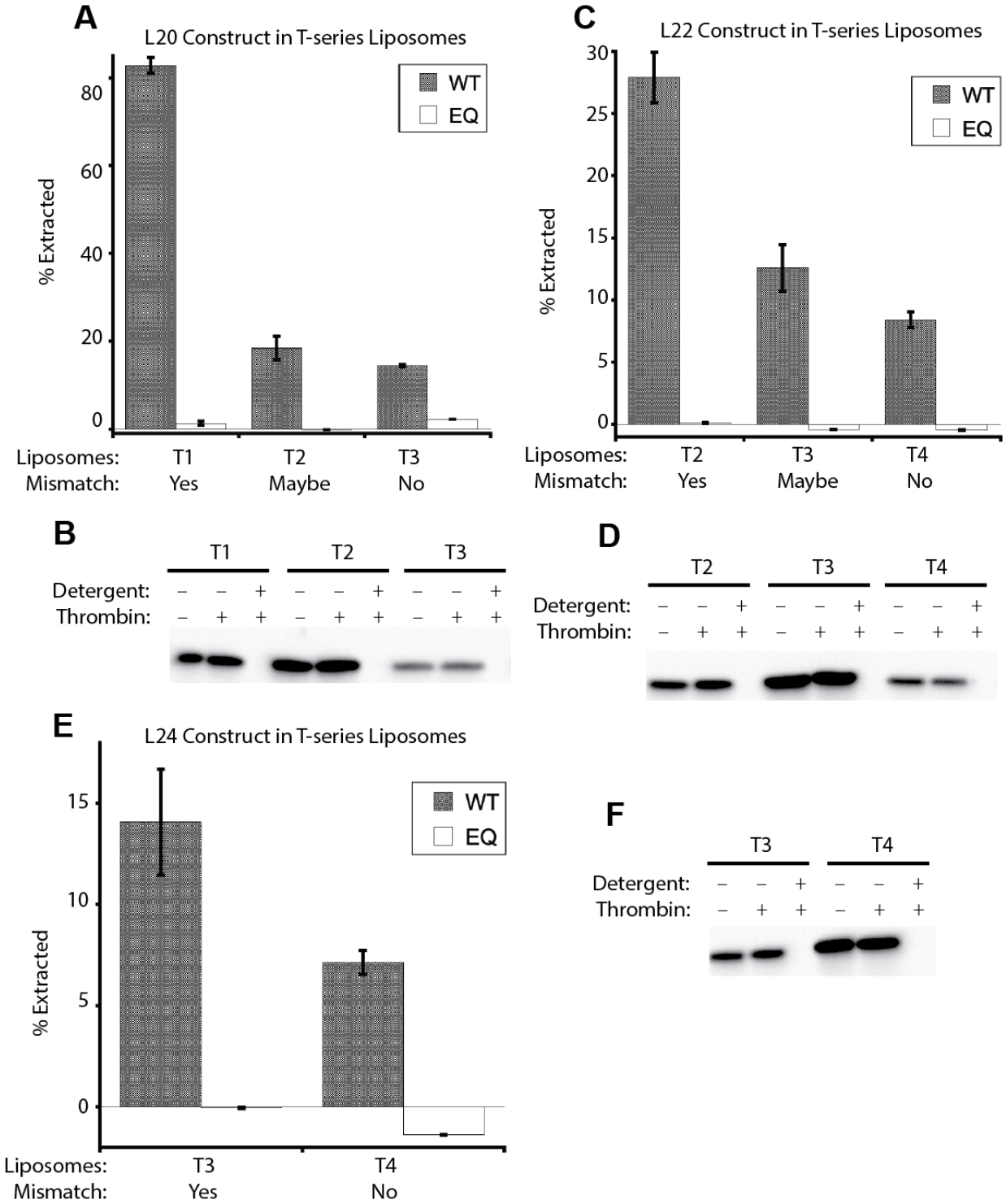

Figure 4: Extraction of L-series substrates in T-series liposomes

A) Extraction of L20 in is most robust when there is a predicted hydrophobic mismatch. L20 substrate was reconstituted in liposomes T1-T3. Based on the length of the TMD and thickness of hydrophobic core of the lipid bilayer, there is a predicted hydrophobic mismatch in T1, a possible mismatch in T2, and no predicted mismatch in T3.

B) Protease protection assay for proteoliposomes in **A**. Anti-HiBiT western blot.

C) Similar to **A**, L22 substrate was reconstituted in liposomes T2-T4. There is a predicted hydrophobic mismatch T2, a possible mismatch in T3, and no predicted mismatch in T4.
D) Protease protection assay for proteoliposomes in **C**. Anti-HiBiT western blot.
E) Similar to **A**, L24 substrate was reconstituted in liposomes T3 and T4. There is a predicted hydrophobic mismatch in T3 and no predicted mismatch in T4.
F) Protease protection assay for proteoliposomes in **E**. Anti-HiBiT western blot.

A

Liposome	Lipid	Conformation
F1	PC (18:1, 18:1)	Trans
F2	PC (18:0, 18:1)	Cis
F3	PC (18:1, 18:1)	Cis
F4	PC (18:2, 18:2)	Cis

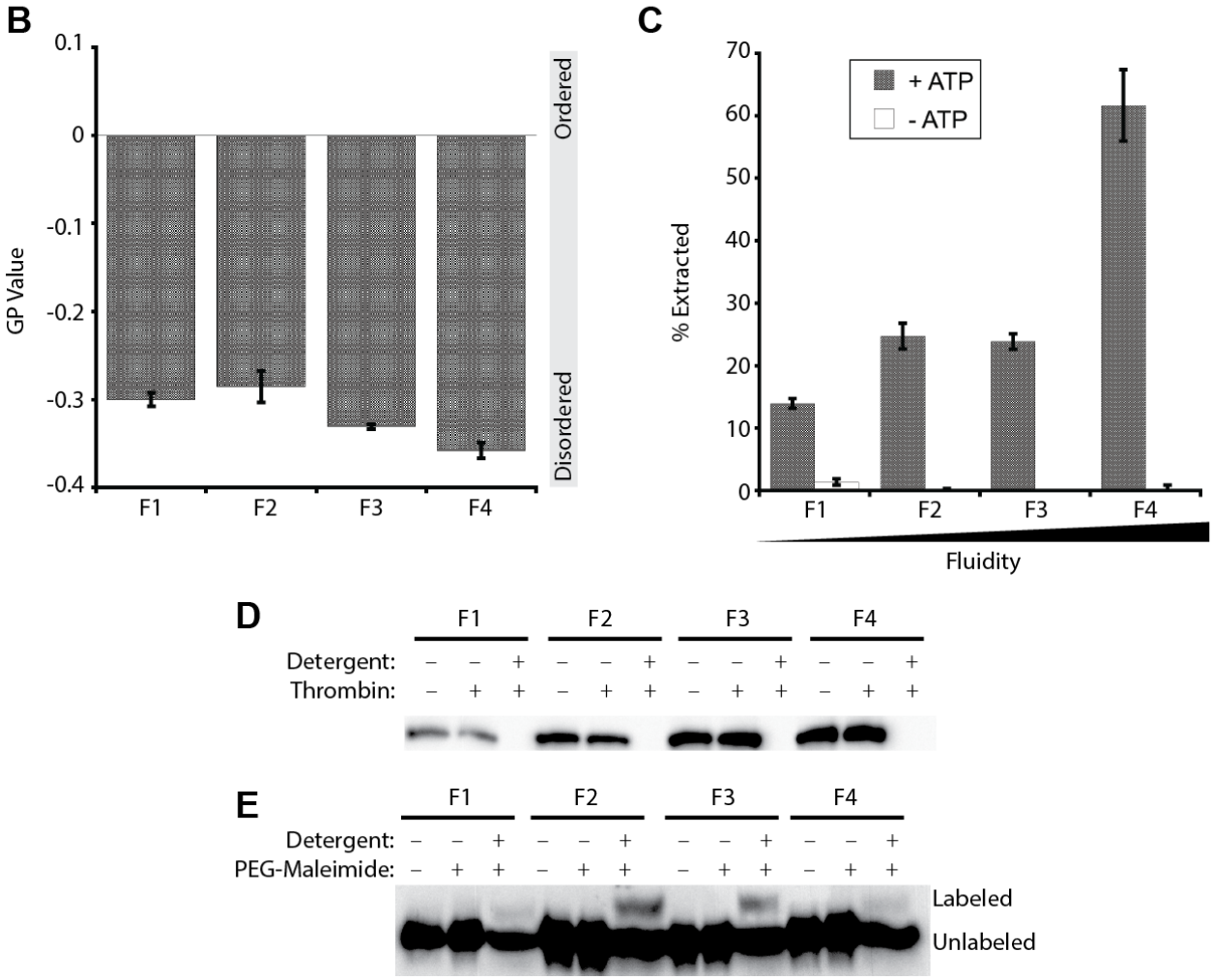

Figure 5: Msp1 extraction activity is enhanced with increasing membrane fluidity

A) Composition of fluidity series liposomes.

B) Lipid packing of F-series liposomes measured by C-Laurdan spectroscopic measurements. Generalized polarization (GP) values range from +1 (most ordered) to -1 (most disordered).

C) Extraction of standard Sumo-Sec22 substrate in F-series liposomes.

D) Protease protection assay for proteoliposomes in **C**.

E) PEG-maleimide labeling shows minimal changes in cysteine reactivity between F-series liposomes.